

Article

A Study on the Mechanical Mechanism of Injection Heat to Increase Production of Gas in Low-Permeability Coal Seam

Hongmei Cheng *, Ning Zhang, Yugui Yang, Weihong Peng and Heng Chen

State Key Laboratory for Geomechanics and Deep Underground Engineering, School of Mechanics and Civil Engineering, China University of Mining and Technology, Xuzhou 221116, China; zhangncumt@163.com (N.Z.); yyg323@163.com (Y.Y.); cnpengweihong@126.com (W.P.); ts18030010a31@cumt.edu.cn (H.C.)

* Correspondence: hmcheng@cumt.edu.cn; Tel.: +86-0516-8359-0666

Received: 13 May 2019; Accepted: 13 June 2019; Published: 18 June 2019



Abstract: This paper puts forward a new mathematical model, which is a coal damage-heat-fluid-solid multi-field coupling theory, in order to reveal the mechanical mechanism of the increase of coal-bed methane recovery through thermal stimulation, and to evaluate its effect. The strain field is introduced to define the damage of coal by considering of the effects of temperature, gas pressure, and mining stress of the coal seam. It is used to quantitatively describe the degree of coal rupture and damage. Additionally, the elastic and damage constitutive equation of coal and rock mass, the governing equation of the temperature field, and the coupling equation of gas diffusion and seepage are established. Based on these equations, the finite element source program is redeveloped by using the FORTRAN language, and a multi-field coupling analysis program is compiled. This program takes the temperature, the gas seepage, and the damage and deformation of coal and rock mass into consideration. The effect of heat injection temperature on gas production efficiency, gas pressure distribution, and effective extraction radius during coal-bed methane mining process is analyzed. The results show that the injection of heat can significantly improve the desorption and diffusion of gas, as well as the gas production rate and the production efficiency of coal-bed methane.

Keywords: injection heat; gas extraction; damage-thermal-gas-solid coupled analysis; damaged coal and rock mass; FORTRAN programs

1. Introduction

The coal seam in China has a strong adsorption, low permeability, and slow desorption rate. Therefore, many coal-bed methane wells have experienced a significant decline in gas production after a period of extraction. Under such conditions, the artificial permeability enhancement technology must be used to improve the gas production per well. At present, hydraulic fracturing, gas displacement technology, blasting technology, thermal stimulation technology, etc. comprise the commonly used methods. For example, Kang [1] suggested the use of liquid CO₂ gasification blasting technology to fracture the coal seam, and results showed that this technology could effectively improve the coal seam permeability, and thus enhance coal-bed methane recovery. Another effective way to improve the production of coal-bed methane is the heat injection technology, which is widely accepted by the academic community [2,3].

Coal is a kind of organic rock that is very sensitive to the temperature. Cai [4] concluded that coal underwent different physical property transformations during the pyrolysis process. The first stage (25–300 °C) is the dry gas stage, during which the moisture and adsorbed gas are desorbed until 200 °C. The low rank coal is thermally decomposed when the temperature of coal is raised from 200 °C to

300 °C. As the temperature reaches 300–550 °C, it is the pyrolysis stage of coal, under which the gas and tar are formed. Yang [5] indicates that the adsorption of methane by coal is an exothermic process. As the temperature of the coal seam increases, the adsorption capacity of coal to methane decreases, and the desorption rate increases. Conversely, the desorption rate decreases. Therefore, the increase of coal seam temperature can enhance the desorption rate of methane. On the other hand, the desorption of methane by coal is an endothermic process. The temperature in the coal seam will locally decrease with the desorption of methane, thus reducing the desorption rate. Lin et al. [6] experimentally determined the adsorption isotherms of coal to methane at different temperatures. They indicated that, with the increase of temperature, the saturated adsorption capacity and adsorption rate of coal-bed methane were significantly reduced. Zhou and Lin [7] showed that the gas adsorption capacity reduced by 8% when the temperature of the coal body increased by one degree Celsius. When compared with the traditional extraction technology, Salmachi [8] found that the gas extraction volume of coal seam was increased by 58% during a period of 12 years after the geothermal water at 80 °C was continuously injected into coal seam, and the maximum gas production rate was 6.8 times higher. Cheraghian [9] studied the effect of The Extractor-Separator hydrocarbon fluids in situ combustion method (ESHF-ISC) parameters, i.e., thermal technology, on the new Thai process performance for conventional and heavy oil reservoirs, and the results showed that ESHF-ISC is more applicable on conventional reservoirs than the Thai method. Therefore, the physical mechanisms of the thermal stimulation in terms of improving coal-bed methane recovery need to be investigated. Wang [10] proposed an equation to express the gas adsorption/desorption as a mathematical function of the reservoir pressure and temperature. Wong [11] claimed that the thermal expansion deformation would be induced if the coal seam is stimulated by heat. The high temperature significantly impacted the thermal deformation, micro crack generation, pore volume, average pore size, porosity, and permeability, as discussed by Akbarzadeh [12]. Permeability is an important parameter in reflecting the difficulty of gas migration in coal seams, and it is also a key parameter for measuring the difficulty of gas extraction. With the increase of temperature, the permeability of coal is related to the adsorption, loading deformation, thermal expansion, and thermal cracking load coupling factors. Accordingly, it is necessary to study the effects of thermal stimulation on reservoir permeability evolution. Zhu et al. [13] comprehensively studied the influence of gas pressure, matrix thermal expansion and deformation, the temperature change on coal porosity, and established a permeability model. Li et al. [14] explored the relationship between permeability and temperature and stress in depth. Wang et al. [15] investigated the permeability of the coal samples by injecting high-temperature nitrogen into boreholes. Shahtalebi et al. [16] studied the feasibility of mining coal-bed methane through thermal stimulation with the resistance method. In conclusion, the mechanism of the thermal stimulation of production improvement can be explained, as follows, the increase of temperature can reduce the adsorption amount of coal-bed methane, changing the microstructure of coal body and improving the permeability of coal seam, thereby increasing the production of coal-bed methane per unit time and achieving the goal of enhancing the extraction of coal-bed methane.

Thermal stimulation for the mining of coal-bed methane is a typical heat-flow-solid multi-field coupling process. At present, little attention has been paid to the damage and fracture of coal and rock mass caused by mining stress, gas migration and temperature change. However, the mechanical properties of coal and rock mass will be changed by the damage and fracture of the material. Such changes will greatly affect the stress field of coal and rock mass and the gas migration. In addition, the internal fissures of coal and rock mass are also critical for gas enrichment and migration. Hence, it is of great importance to understand the development degree and distribution of damage and fracture of coal and rock mass. Based on damage mechanics, this paper attempts to establish a theoretical model of damage-heat-gas-solid multi-field coupling of coal and rock mass in construction engineering. The FORTRAN language is applied to compile large-scale procedures to calculate and analyze the engineering application of coal-bed methane mining by while using the thermal stimulation. The

influence of different heating temperatures on the dynamic evolution process of gas pressure and the mining efficiency of coal-bed methane is deeply studied.

2. Coal and Rock Damage-Heat-Gas-Solid Multi-Field Coupling Theory

2.1. Damage and Deformation Control Equation of Coal and Rock Mass

Mining stress, gas migration, and temperature change that are caused by industrial construction or mining activities in deep coal and rock mass will cause the fracture and damage of coal and rock mass. The damage variable that relates to strains is introduced in order to give a quantitative description of the damage degree of coal and rock mass. It can be defined under uniaxial compressive stress [17] as follows:

$$\omega = \begin{cases} 0 & 0 < \varepsilon \leq \varepsilon_f \\ \frac{\varepsilon_u(\varepsilon - \varepsilon_f)}{\varepsilon(\varepsilon_u - \varepsilon_f)} & \varepsilon_f < \varepsilon \leq \varepsilon_u \end{cases} \quad (1)$$

where ω is the damage variable, ε_f is the threshold strain of coal damage evolution, and ε_u is the ultimate strain of damage evolution of coal and rock mass.

When the coal and rock mass is in the three direction stress state [18], the three principal strains are known to be ε_1 , ε_2 , and ε_3 , respectively,

The equivalent total strain is

$$\varepsilon = \sqrt{\varepsilon_1^2 + \varepsilon_2^2 + \varepsilon_3^2} \quad (2)$$

The equivalent tensile strain and compressive strain can be given as follows respectively:

$$\varepsilon_t = \sqrt{\sum \varepsilon_i^2} (\varepsilon_i > 0) \quad (3)$$

$$\varepsilon_c = \sqrt{\sum \varepsilon_j^2} (\varepsilon_j < 0) \quad (4)$$

It is assumed that the damage of coal and rock mass is irreversible. Under the condition of three direction compression, the total damage of coal and rock mass can be expressed by the equivalent tensile damage and the equivalent pressure damage, as follows:

$$\omega = \left(\frac{\varepsilon_t}{\varepsilon}\right)^2 \omega_t + \left(\frac{\varepsilon_c}{\varepsilon}\right)^2 \omega_c \quad (5)$$

Experimental research shows that, under normal conditions, the deformation and strength characteristics of most types of rock mass belong to the category of brittle failure. Therefore, it is assumed that the coal and rock damage is mainly caused by deviatoric stress. The damage constitutive equation of rock mass can be expressed, as follows [19]:

$$\sigma_{ij} = (1 - \omega) E_{ijkl} \varepsilon_{kl}^e + \frac{\omega}{3} \delta_{ij} E_{ppkl} \varepsilon_{kl}^e \quad (6)$$

where E_{ijkl} is the material parameters of coal and rock mass, ε_{kl}^e is the elastic strain, and δ_{ij} is the Kronecker symbol.

The matrix form of Formula (6) can be written, as follows

$$\sigma = \tilde{\mathbf{D}} \varepsilon^e \quad (7)$$

where $\tilde{\mathbf{D}}$ is the elastic matrix of coal and rock damage, which is related to elastic modulus E , Poisson's ratio μ , and damage variable ω .

2.2. Effective Stress Theory of Coal Containing Gas

It is assumed that coal is a dual medium with pore-fracture, and the pores and coal skeleton particles are treated as a whole. Under the action of external force F_z , the supporting stress σ'_z will be generated at the contact point of the coal particles. At the same time, the adsorption expansion deformation and the thermal expansion deformation are converted into adsorption expansion stress σ^{ad} and thermal stress σ^t , respectively.

When there is no external constraint, the surface tension of the coal particles decreases after the gas is adsorbed. The volume of the coal particles is expanded, and a part of the surface energy and heat of adsorption are converted into elastic deformation energy. Therefore, the volumetric strain of the adsorption expansion of coal particles in free space can be expressed as [20]:

$$\varepsilon'_v = \frac{2a\rho_v RT(1-2\mu)\ln(1+bp)}{EV_m} \quad (8)$$

Hooke's law can be used to describe the relationship between the adsorption expansion stress and strain at the contact point when assuming that the coal particle is under unidirectional compression at the contact point, which is, one-third of the volumetric strain ε'_v of the adsorption expansion in free space is converted into adsorption expansion stress σ^{ad} .

$$\sigma^{ad} = E\varepsilon^{ad} = \frac{2a\rho_v RT(1-2\mu)\ln(1+bp)}{3V_m} \quad (9)$$

where a is the ultimate adsorption capacity of combustibles per unit mass under reference pressure, b is the adsorption constant, μ is the Poisson's ratio of coal seam, and ρ_v is the apparent density of coal body; R is the gas constant of coal seam methane, T is the temperature of coal seam, and V_m is the molar volume of the gas under standard conditions.

The relationship between the thermal expansion deformation of coal particles and temperature increment can be expressed, as follows, while assuming that the coal is elastic and isotropic [21]:

$$\varepsilon^t = \alpha_s \Delta T \quad (10)$$

Subsequently, the thermal expansion stress of coal is as follows

$$\sigma^t = E\alpha_s \Delta T \quad (11)$$

where ε^t is the volumetric strain caused by thermal expansion of the coal body, σ^t is the uniform thermal expansion stress, α_s is the uniform thermal expansion coefficient of the coal seam volume, and ΔT is the temperature increment of the coal seam.

Free gas is dominant on the surface of coal cracks. The total stress of coal body is composed of pore pressure, adsorption expansion stress, thermal stress, and effective stress of the fracture section. Among them, the effective stress determines the deformation and strength of the coal containing gas. The effective stress of coal body can be written according to Terzaghi's effective stress principle [20], as follows:

$$\sigma'_{ij} = \sigma_{ij} + \sigma^{ad} + \alpha p + \sigma^t \quad (12)$$

Namely,

$$\sigma'_{ij} = \sigma_{ij} + (\alpha + \beta)p\delta_{ij} + E\alpha_s \Delta T \quad (13)$$

where $\beta = \frac{2a\rho_v RT(1-2\mu)\ln(1+bp)}{3V_m p}$, σ'_{ij} is the effective stress, σ_{ij} is the total stress, p is the pore pressure, and α is the Biot coefficient [22], $\alpha = 1 - K/K_s$, $\alpha \leq 1$, K is the bulk modulus of coal mass, and K_s is the bulk modulus of coal particles.

2.3. Damage and Deformation Control Equation of Coal Containing Gas

According to the theory of elasticity, three-dimensional equilibrium differential equation of coal and rock mass is

$$\sigma'_{ij,j} + F_i = 0 \quad (14)$$

The relation between strain and displacement of coal and rock mass is described by the geometric equation, as follows

$$\varepsilon_{ij} = \frac{1}{2}(u_{i,j} + u_{j,i}) \quad (15)$$

Substituting the Formulas (6) and (15) into the Equation (13), then substituting the Formula (13) into the Formula (14), the deformation control equations of the damaged coal and rock mass, which relate to coal seam temperature and gas pressure are obtained, as follows:

$$\begin{aligned} B \frac{\partial^2 u}{\partial x^2} + C \left(\frac{\partial^2 u}{\partial y^2} + \frac{\partial^2 u}{\partial z^2} \right) + (A + C) \left(\frac{\partial^2 v}{\partial x \partial y} + \frac{\partial^2 w}{\partial x \partial z} \right) - \frac{\partial(\alpha p + \beta p)}{\partial x} - E \alpha_s \cdot \frac{\partial T}{\partial x} &= 0 \\ B \frac{\partial^2 v}{\partial y^2} + C \left(\frac{\partial^2 v}{\partial x^2} + \frac{\partial^2 v}{\partial z^2} \right) + (A + C) \left(\frac{\partial^2 u}{\partial y \partial x} + \frac{\partial^2 w}{\partial y \partial z} \right) - \frac{\partial(\alpha p + \beta p)}{\partial y} - E \alpha_s \cdot \frac{\partial T}{\partial y} &= 0 \\ B \frac{\partial^2 w}{\partial z^2} + C \left(\frac{\partial^2 w}{\partial y^2} + \frac{\partial^2 w}{\partial x^2} \right) + (A + C) \left(\frac{\partial^2 u}{\partial z \partial x} + \frac{\partial^2 v}{\partial z \partial y} \right) - \frac{\partial(\alpha p + \beta p)}{\partial z} - E \alpha_s \cdot \frac{\partial T}{\partial z} - \rho_v g &= 0 \end{aligned} \quad (16)$$

where, $A = \frac{E\mu}{(1+\mu)(1-2\mu)} + \frac{E}{1+\mu} \frac{\omega}{3}$, $B = \frac{E(1-\mu)}{(1+\mu)(1-2\mu)} - \frac{E}{1+\mu} \frac{2\omega}{3}$, $C = \frac{(1-\omega)E}{2(1+\mu)}$.

The displacement can be obtained by solving Formula (13). The strain and volumetric strain at various points in coal body under thermal stimulation can be obtained according to the geometric Equation (12) of coal and rock mass.

2.4. Migration Theory of Gas in Coal Seam

2.4.1. Gas Content Equation in Coal Seam

The gas exists in the coal seam in two states: one is adsorption state and the other is free state. The gas in the adsorption state obeys the Langmuir equation and the free state gas obeys the ideal gas equation of state [20]. The mass concentration C' of the absorbed gas and the density ρ of free coal-bed methane can be expressed, as follows:

$$C' = \frac{abcpp_n M_g}{(1 + bp)RT} \quad (17)$$

$$\rho = \frac{pM_g}{RT} \quad (18)$$

The product of free gas density and porosity is the gas concentration of the free state in coal seam, so the total mass concentration M of gas in coal seam can be expressed, as follows

$$M = \frac{abcpp_n M_g}{(1 + bp)RT} + \frac{\varphi p M_g}{RT} \quad (19)$$

where p is the absorption equilibrium pressure, c is the mass of combustibles per unit volume of coal, p_n is normal atmosphere, φ is porosity of coal seam, and M_g is the mole mass of methane.

2.4.2. Control Equation of Gas Migration

Coal seam is a typical pore-fissure medium, which is mainly composed of matrix, pore, and fissure. The pore structures in coal seams include large poles, medium pores, and micro-pores. Therefore, it is considered that the gas migration in large and medium pores obeys Fick diffusion, and the gas

migration in micro pores obeys Knudsen diffusion [23]. However, in the fracture system, the free gas has nonlinear seepage movement [24,25].

Fick Diffusion Equation

The gas emission process from the large and medium pores in the coal seam is regarded as the diffusion movement of gas in the porous medium, which can be expressed by the Fick diffusion law, as follows:

$$m_f = -D_f \nabla C' \quad (20)$$

where, m_f is the Fick diffusion flux vector, the Fick diffusion coefficient D_f can be given, as follows [26]:

$$D_f = \frac{1}{3} \sqrt{\frac{8k_B T}{\pi m}} \frac{k_B T}{\sqrt{2\pi} \delta^2 p} = 2.196 \times 10^{-4} T^{\frac{3}{2}} p^{-1} \quad (21)$$

The effective Fick diffusion coefficient can be given when considering the effects of seam porosity and pore tortuosity on the gas diffusion, as follows [27]:

$$D_f^{eff} = \frac{\varphi}{\tau} D_f \quad (22)$$

where, $k_B = 1.38 \times 10^{-23}$ J/K is the Boltzmann constant, m is the methane molecular mass, T is coal seam temperature, D_f^{eff} is effective Fick diffusion coefficient, and τ is the pore tortuosity of the micro pores along the diffusion direction of methane molecules.

Knudsen Diffusion Equation

The migration of gas in the micro-pore of coal seam can be regarded as Knudsen diffusion. Ignoring the effects of gas viscosity, and the mass flux equation of Knudsen diffusion of gas in micro-pores is given, as follows [28]:

$$m_k = -\frac{D_k M_g}{RT} \nabla p \quad (23)$$

where,

$$D_k = \frac{d_p}{3} \sqrt{\frac{8RT}{\pi m}} = 12.125 T^{0.5} d_p \quad (24)$$

$$D_k^{eff} = \frac{\varphi}{\tau} \frac{d_p}{3} \sqrt{\frac{8RT}{\pi m}} \quad (25)$$

where, m_k is the Knudsen diffusion flux vector, D_k is the Knudsen diffusion coefficient, d_p is the pore diameter, m is of methane molecular mass, D_k^{eff} is the Knudsen effective diffusion coefficient, and ∇p is the gas pressure gradient.

Nonlinear Seepage Equation

In general, Darcy seepage law represents the migration of free gas in coal seam, as follows

$$\mathbf{V} = -\frac{k}{\mu_g} \nabla p \quad (26)$$

where, \mathbf{V} is the seepage velocity vector of free gas, k is the permeability of coal seam, μ_g is the dynamic viscosity of coal bed gas, and p is the free pressure of free gas in the fracture system.

When the average molecular free path of methane is close to the pore size of coal body, there will be a slippage that is caused by the Klinkenberg effect. At this time, the speed of methane molecules on the channel wall is not zero. The research shows that the Klinkenberg effect has great influence on the seepage of gas in coal seam, and it can more accurately reflect the true seepage state of gas in the coal

seam. Therefore, on the basis of the linear Darcy seepage law, an additional term of velocity is added to consider the slippage effect. Therefore, the nonlinear seepage equation of gas in coal seam can be concluded, as follows:

$$\mathbf{V} = -\frac{k}{\mu_g} \left(1 + \frac{b_k}{p}\right) \nabla p \quad (27)$$

where, b_k is the Klinkenberg coefficient, and its calculation formula is given by Jones, as follows [29]:

$$b_k = 0.95k^{-0.33} \quad (28)$$

2.4.3. Continuity Equation of Gas Migration in Coal Seam

(1) The continuity equation of diffusion motion in the pore system

In the pore system, the gas diffusion reduces the content of the adsorbed gas. The continuity equation of gas diffusion motion in the pore system can be obtained according to the principle of mass conservation, as follows:

$$\frac{\partial C'}{\partial t} = -\nabla \cdot (\mathbf{m}_f + \mathbf{m}_k) - q \quad (29)$$

Substituting the Formulas (20) and (23) into Equation (29), the continuity equation of the diffusive motion in the pore system is obtained as

$$\frac{abc p_n M_g}{(1+bp)^2 RT} \frac{\partial p}{\partial t} = \nabla \cdot \left(D_f^{eff} \frac{abc p_n M_g}{(1+bp)^2 RT} \nabla p + D_k^{eff} \frac{M_g}{RT} \nabla p \right) - q \quad (30)$$

(2) The continuity equation of the seepage movement in the fracture system

In the fracture system, assuming that v_x , v_y , and v_z are the components of the gas seepage velocity vector v in the direction of each coordinate axis, respectively, q is a positive quality exchange source term and t is time. According to the principle of mass conservation, the continuity equation of gas seepage movement can be obtained, as follows:

$$\frac{\partial(\varphi\rho)}{\partial t} = -\left[\frac{\partial(\rho v_x)}{\partial x} + \frac{\partial(\rho v_y)}{\partial y} + \frac{\partial(\rho v_z)}{\partial z} \right] + q \quad (31)$$

Substituting the Formulas (18) and (27) into the Equation (31), the continuity equation of seepage motion in the fissure system is obtained, as follows

$$\frac{M_g}{RT} \frac{\partial(\varphi p)}{\partial t} = \nabla \cdot \left(\frac{M_g}{RT} \frac{k}{\mu_g} (p + 0.95k^{-0.33}) \nabla p \right) + q \quad (32)$$

(3) The continuity equation of coupling motion of the gas diffusion and seepage

The above equations are gained by dividing the gas flow into diffusion motion and seepage motion in two open systems, respectively. If the adsorption, desorption and diffusion of gas are regarded as a system, the desorption of gas makes the adsorption gas be transformed into free state and enter the seepage system through the diffusion motion of pores. The mass transfer is completed by the mass exchange source in the two systems. The concentration controls the gas diffusion and seepage and they affect each other. A coupling effect happens between the gas diffusion and the seepage. As the gas adsorption and desorption only causes the change in the gas state, it has no effect on the change of gas quality. Equations (30) and (32) can be added to the flow continuity equation with the interaction of diffusion and seepage, as follows:

$$\frac{abc p_n M_g}{(1+bp)^2 RT} \frac{\partial p}{\partial t} + \frac{M_g}{RT} \frac{\partial(\varphi p)}{\partial t} = \nabla \cdot \left(D_f^{eff} \frac{abc p_n M_g}{(1+bp)^2 RT} \nabla p + D_k^{eff} \frac{M_g}{RT} \nabla p \right) + \nabla \cdot \left(\frac{M_g}{RT} \frac{k}{\mu_g} (p + 0.95k^{-0.33}) \nabla p \right) \quad (33)$$

The equation is unfolded and collated, as follows:

$$\left[\varphi + \frac{abc p_n}{(1+bp)^2} \right] \frac{\partial p}{\partial t} + p \frac{\partial \varphi}{\partial t} - \frac{k}{\mu_g} \nabla p \nabla p - \left(p + 0.95 \cdot 0.67 k^{-0.33} \right) \frac{\nabla k \nabla p}{\mu_g} - \left(\frac{D_f^{eff} abc p_n}{(1+bp)^2} + p \frac{k}{\mu_g} + 0.95 \cdot \frac{k^{0.67}}{\mu_g} + D_k^{eff} \right) \nabla^2 p = 0 \quad (34)$$

2.5. Control Equation of Temperature Field of the Coal Containing Gas

The coal containing gas will be deformed under the action of heat and external force, while considering non-isothermal seepage, taking the coal-bed methane micro-element as the analysis object, the law of conservation of energy shows, as follows [30]:

$$\frac{\partial(\varphi \rho h_g)}{\partial t} + \nabla \cdot (\rho h_g \mathbf{V}) - \varphi \nabla \cdot (k_g \nabla T) = \varphi Q_{T_g} \quad (35)$$

where k_g is the thermal conductivity of gas, $h_g = c_p T$ is the specific enthalpy of unit mass gas, c_p is specific heat at constant pressure, and \mathbf{V} is seepage velocity of gas.

In the same way, taking the coal skeleton micro-element as the analysis object, the law of conservation of energy shows:

$$\frac{\partial(\rho_s h_s)}{\partial t} + T \alpha_s K \frac{\partial \varepsilon_v}{\partial t} - \nabla \cdot (k_s \nabla T) + \frac{q_{st}}{M_g} \frac{\partial C'}{\partial t} = Q_{T_s} \quad (36)$$

where, ρ_s is density of the coal skeleton, α_s is the thermal expansion coefficient, $h_s = c_s T$ is the specific enthalpy of unit mass coal body, c_s is heat capacity of coal body, k_s is heat conduction coefficient of coal skeleton, Q_{T_s} is the strength of coal body skeleton heat source, and q_{st} is equal amount of adsorption heat.

It is assumed that the coal and gas always keep in the state of heat balance, the temperature field control equation with gas coal is obtained by adding (35) and (36), as follows:

$$c_h \frac{\partial T}{\partial t} + T \alpha_s K \frac{\partial \varepsilon_v}{\partial t} + \nabla \cdot (\rho h_g \mathbf{V}) - \nabla \cdot (k_t \nabla T) + \frac{q_{st} abc p_n}{(1+bp)^2 RT} \frac{\partial p}{\partial t} = Q_T \quad (37)$$

where, $c_h = \rho_s c_s + \varphi \rho c_g$ is heat capacity for coal containing gas, $k_t = k_s + \varphi k_g$ is heat conduction coefficient for coal containing gas, and $Q_T = Q_{T_s} + \varphi Q_{T_g}$ is the total heat source strength.

Substituting the Formulas (18) and (27) into the Equation (37), the temperature field control equation of coal containing gas is obtained, as follows

$$\begin{aligned} & c_h \frac{\partial T}{\partial t} + T \alpha_s K \frac{\partial \varepsilon_v}{\partial t} - \rho c_p \frac{k}{\mu_g} \left(1 + \frac{0.95 k^{-0.33}}{p} \right) \nabla p \nabla T \\ & - \rho c_p T \left(\frac{k}{\mu_g} \left(1 + \frac{0.95 k^{-0.33}}{p} \right) \cdot \nabla^2 p + \left(1 + \frac{0.95 k^{-0.33}}{p} \right) \frac{\nabla p \cdot \nabla k}{\mu_g} \right) \\ & - k_t \nabla^2 T + \frac{q_{st} abc p_n}{(1+bp)^2 RT} \frac{\partial p}{\partial t} = Q_T \end{aligned} \quad (38)$$

2.6. Evolution Mechanism of Permeability of Damaged Coal Mass

With the increase of temperature, the coal permeability will greatly change under the coupling effect of compression, damage and fracture, thermal expansion, and thermal adsorption of coal body. Therefore, it is necessary to establish relevant quantitative indicators to explain the stimulation effect of temperature on permeability, and to further explore the effects of these coupling effects on the evolution of coal permeability and the thermal stimulation effect of coal-bed methane reservoirs.

Dr. Teng T. of our research group tested the permeability of the heat-stimulated coal sample, and obtained the permeability of the thermal stimulated coal samples by using N_2 at 1 MPa and CO_2 at 7 MPa, respectively. Figure 1 shows the results [31].

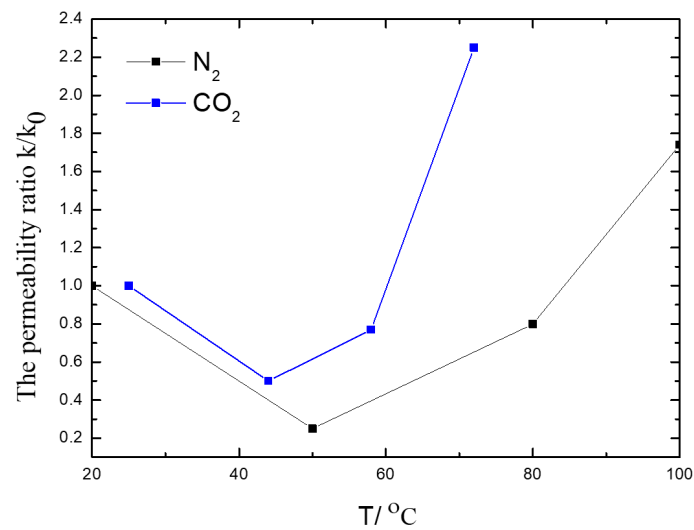


Figure 1. The permeability ratio curve with temperature.

It can be seen from Figure 1 that the permeability of thermal stimulation coal sample changes with temperature in a “U” shape. At the beginning of heating, the internal crack of the coal body is compacted due to the expansion deformation of the coal matrix, resulting in a corresponding decrease of the permeability of the coal body. As the temperature continues to rise, a large number of adsorbed gases in coal samples are desorbed, which eventually leads to the shrinkage of the coal matrix and the permeability can be greatly improved. However, the effect of stress field on permeability is not taken into account in the above experiments. Therefore, this thesis intends to comprehensively consider the effects of temperature, gas adsorption and desorption, stress, damage, and rupture to establish a mechanical model of coal permeability.

According to the analysis in the previous section, it is assumed that one-third of the volumetric strain of the adsorbed expansion in the free space is converted into the expansion stress at the contact point. The other two-thirds is the inward adsorption expansion strain that changes the volume of the fracture, which can be expressed, as follows:

$$\varepsilon_p = \frac{4a\rho_v RT(1-2\mu)\ln(1+bp)}{3EV_m} \quad (39)$$

where ε_p is an inward adsorption expansion strain and E is the modulus of elasticity associated with coal damage.

According to the equivalent strain principle, the relationship between the coal elastic modulus and the damage degree can be expressed, as follows

$$E = (1-\omega)E_0 \quad (40)$$

where E_0 is the initial elastic modulus of coal seam.

Porosity is one of the important parameters for the study of gas migration, and it can be defined, as follows [20]:

$$\varphi = \frac{V_\varphi}{V_v} = \frac{(V_{\varphi 0} - \Delta V_p + \Delta V_v - \Delta V_t)/V_{v0}}{(V_{v0} + \Delta V_v)/V_{v0}} = \frac{\varphi_0 - \varepsilon_p + \varepsilon_v - \varepsilon_v^t}{1 + \varepsilon_v} \quad (41)$$

where $V_{\varphi 0}$ is the volume of the pore before deformation, V_φ is the volume of the pore after deformation, ΔV_p is the amount of volume change caused by inward adsorption expansion deformation, ΔV_t is the amount of volume change caused by inward thermal expansion deformation, and ΔV_v is the amount of apparent volume change of the coal seam.

In the actual project, the coal body will continue to be damaged and ruptured with the artificial extraction activity, so the permeability of the coal has a tendency to increase by two to four orders of magnitude. Therefore, this section introduces porosity to represent damage and to provide a quantitative description of the rupture degree of coal body, as follows [32]:

$$\omega = \frac{\varphi - \varphi_0}{\varphi_s - \varphi_0} = \frac{\frac{\varphi_0 - \varepsilon_p + \varepsilon_v - \varepsilon_v^t}{1 + \varepsilon_v} - \varphi_0}{\frac{\varphi_0 - \varepsilon_p + \varepsilon_v^s - \varepsilon_v^t}{1 + \varepsilon_v^s} - \varphi_0} = \frac{1 + \varepsilon_v^s}{1 + \varepsilon_v} \cdot \frac{(1 - \varphi_0)\varepsilon_v - \varepsilon_p - \varepsilon_v^t}{(1 - \varphi_0)\varepsilon_v^s - \varepsilon_p - \varepsilon_v^t} \quad (42)$$

where φ_0 is initial porosity, φ_s is porosity of broken coal and rock, and ε_v^s is the ultimate volumetric strain of fracture coal mass.

The permeability is an important parameter to reflect the difficulty for gas migration in coal seam and is the key parameter for measuring the gas drainage difficulty. The Kozeny-Carman equation provides the permeability, as follows [23]:

$$k = \frac{\varphi^3}{c_0(1 - \varphi)^2 S^2} \quad (43)$$

where, c_0 is a dimensionless number, which generally taken 5, and S is the specific surface area.

According to Equations (41)–(43), the coal permeability related to stress, damage, temperature, and gas pressure can be obtained, as follows:

$$k = \frac{k_0(1 - \varphi_0)^2}{1 + \varepsilon_v^s} \left(\frac{(1 + \varepsilon_v^s)\varphi_0 + \omega((1 - \varphi_0)\varepsilon_v^s - \varepsilon_p - \varepsilon_v^t)}{(1 + \varepsilon_v^s)(1 - \varphi_0) - \omega((1 - \varphi_0)\varepsilon_v^s - \varepsilon_p - \varepsilon_v^t)} \right)^3 \quad (44)$$

2.7. Heat-Gas-Solid Coupling Model of Damaged Coal Seam

If the dynamic evolution model of the porosity and permeability of damaged coal and rock mass is brought into the multi-physical field control equation, and a multi-physical field coupling model, including the coal and rock damage field, the temperature field, and the gas seepage field, can be obtained.

In Formulas (41), the partial derivative of porosity to time can be obtained, as follows

$$\frac{\partial \varphi}{\partial t} = \frac{(1 - \varphi_0)\varepsilon_v^s - \varepsilon_p - \varepsilon_v^t}{1 + \varepsilon_v^s} \cdot \frac{\partial \omega}{\partial t} - \frac{\omega}{1 + \varepsilon_v^s} \cdot \frac{4a\rho_v RT(1 - 2\mu)}{3(1 + bp)EV_m} \cdot \frac{\partial p}{\partial t} - \frac{2\alpha_s \omega}{1 + \varepsilon_v^s} \cdot \frac{\partial T}{\partial t} \quad (45)$$

Substituting the Equations (41) and (45) into the Formulas (34), the governing equation of coal-bed methane flow under multi-physical field coupling is obtained, as follows

$$\begin{aligned} & \left[\frac{\varphi_0(1 + \varepsilon_v^s - \omega\varepsilon_v^s) + \omega(\varepsilon_v^s - \varepsilon_p - \varepsilon_v^t)}{1 + \varepsilon_v^s} + \frac{abc p_n}{(1 + bp)^2} - p \frac{\omega}{1 + \varepsilon_v^s} \cdot \frac{4a\rho_v RT(1 - 2\mu)}{3(1 + bp)EV_m} \right] \frac{\partial p}{\partial t} + \\ & p \left[\frac{(1 - \varphi_0)\varepsilon_v^s - \varepsilon_p - \varepsilon_v^t}{1 + \varepsilon_v^s} \cdot \frac{\partial \omega}{\partial t} - \frac{2\alpha_s \omega}{1 + \varepsilon_v^s} \cdot \frac{\partial T}{\partial t} \right] - \frac{k}{\mu_g} \nabla p \nabla p - (p + 0.95 \times 0.67k^{-0.33}) \cdot \\ & \frac{\nabla k \nabla p}{\mu_g} - \left[\frac{D_f^{eff} abc p_n}{(1 + bp)^2} + p \frac{k}{\mu_g} + 0.95 \cdot \frac{k^{0.67}}{\mu_g} + D_k^{eff} \right] \nabla^2 p = 0 \end{aligned} \quad (46)$$

When considering Equations (38) and (42), the governing equations of the temperature field under the coupling of multiple physical fields is obtained, as follows

$$\begin{aligned} & \rho_s c_s + \rho c_g \frac{\varphi_0(1+\varepsilon_v^s - \omega \varepsilon_v^s) + \omega(\varepsilon_v^s - \varepsilon_p - \varepsilon_v^t)}{1+\varepsilon_v^s} \frac{\partial T}{\partial t} + T \alpha_s K \frac{\partial \varepsilon_v}{\partial t} \\ & - \rho c_p T \left(\frac{k}{\mu_g} \left(1 + \frac{0.95k^{-0.33}}{p} \right) \cdot \nabla^2 p + \left(1 + \frac{0.95k^{-0.33}}{p} \right) \frac{\nabla p \cdot \nabla k}{\mu_g} \right) \\ & - \left(k_s + \frac{\varphi_0(1+\varepsilon_v^s - \omega \varepsilon_v^s) + \omega(\varepsilon_v^s - \varepsilon_p - \varepsilon_v^t)}{1+\varepsilon_v^s} k_g \right) \nabla^2 T + \frac{q_{st} a b c p_n}{(1+bp)^2 RT} \frac{\partial p}{\partial t} = Q_T \end{aligned} \tag{47}$$

3. Numerical Solution of Damage-Heat-Gas-Solid Coupling Model of Coal and Rock Mass

3.1. Finite Element Equation for Calculating the Damage and Deformation of Coal and Rock

3.1.1. Calculation of Equivalent Nodal Load

When considering the effect of gravity, boundary distribution force, and initial stress, the general expression of element equivalent nodal load is:

$$P^e = P_f^e + P_S^e + P_{\sigma_0}^e + P_{\sigma_t}^e \tag{48}$$

where P_f^e , P_S^e , $P_{\sigma_0}^e$, and $P_{\sigma_t}^e$ are the equivalent nodal load corresponding to the gravity of the unit f , the boundary distribution force T , and the initial gas adsorption expansion stress σ_0 in the unit and the initial thermal stress σ_t in the unit, respectively

$$P_f^e = - \int_{V_e} N^T \rho_v g dV \tag{49}$$

$$P_S^e = \int_{S_e^s} N^T T dS \tag{50}$$

$$P_{\sigma_0}^e = - \int_{V_e} B^T \sigma_0 dV = - \int_{V_e} B^T \frac{2a \rho_v RT (1 - 2\mu) \ln(1 + bp_0)}{3V_m} dV \tag{51}$$

$$P_{\sigma_t}^e = - \int_{V_e} B^T \sigma_t dV = - \int_{V_e} B^T E \alpha_s (T - T_s) dV \tag{52}$$

where N^T is the transposition matrix of unit shape function and B^T is the transposition matrix of unit strain matrix.

3.1.2. Calculation of Damage Stiffness Matrix of Coal and Rock

When considering the nonlinear problems and the complex loading methods often encountered in actual coal mining operations, the incremental loading method is used to solve this problem step by step. First, according to the Equation (7), the elastic constitutive equation of damage coal and rock mass can be expressed in incremental form, as follows

$$d\sigma_{ij} = \widetilde{D}_{ijkl} d\varepsilon_{kl}^e + \varepsilon_{kl}^e \frac{\partial \widetilde{D}_{ijkl}}{\partial \omega} d\omega \tag{53}$$

When considering the k step of calculation, the incremental matrix form of the Equation (53) can be obtained, as follows:

$$\Delta \sigma_k = \widetilde{D}_k \Delta \varepsilon_k^e + \Delta \widetilde{D}_k \varepsilon_k^e \tag{54}$$

where $\Delta\sigma_k$ is the stress increment matrix of the k step of calculation, $\Delta\varepsilon_k^e$ is the stress increment matrix of the k step of calculation, and $\Delta\tilde{D}_k$ is the damage increment matrix of the k step of calculation. For unit i :

$$(\Delta\tilde{D}_k)_i = \frac{\partial(\Delta\tilde{D}_k)_i}{\partial(\omega_k)_i} (\Delta\omega_k)_i \quad (55)$$

where $(\Delta\omega_k)_i = (\omega_k)_i - (\omega_{k-1})_i$, which can be calculated by the damage evolution Equation (5), and the elastic increment matrix of damage can be obtained by the Formula (7), as follows:

$$\Delta\tilde{D} = \frac{\partial\tilde{D}}{\partial\omega} \Delta\omega = \begin{bmatrix} B_1 & A_1 & A_1 & 0 & 0 & 0 \\ A_1 & B_1 & A_1 & 0 & 0 & 0 \\ A_1 & A_1 & B_1 & 0 & 0 & 0 \\ 0 & 0 & 0 & C_1 & 0 & 0 \\ 0 & 0 & 0 & 0 & C_1 & 0 \\ 0 & 0 & 0 & 0 & 0 & C_1 \end{bmatrix} \Delta\omega \quad (56)$$

where $A_1 = \frac{E}{3(1+\mu)}$, $B_1 = -\frac{2E}{3(1+\mu)}$, $C_1 = \frac{-E}{2(1+\mu)}$.

According to the principle of virtual work, in the k calculation step, the virtual works of the element stress increment and nodal load increment, respectively, in the computation domain are equal in any virtual displacement. The incremental form equilibrium equation can be obtained, as follows

$$\sum_{\Omega} \int B_k^T \Delta\sigma_k d\Omega - \Delta f_k = 0 \quad (57)$$

where B_k , $\Delta\sigma_k$, and Δf_k are the strain matrix, the stress increment matrix, and the load increment matrix of the element in the k calculation step, respectively.

Substituting the Equation (54) into Equation (57), the finite element equation for damage and deformation of coal and rock mass can be obtained, as follows

$$\tilde{K}_k \Delta a_k = \Delta f_k + \Delta f_k^d \quad (58)$$

where \tilde{K}_k is the damage stiffness matrix of the unit, Δa_k is the displacement increment matrix of the unit, and Δf_k^d is the additional forces that are generated by the evolution of coal and rock damage, so its calculation formulas are as follows

$$\tilde{K}_k = \sum_{\Omega} \int B_k^T \tilde{D}_k B_k d\Omega \quad (59)$$

$$\Delta f_k^d = -\sum_{\Omega} \int B_k^T \Delta\tilde{D}_k \varepsilon_k^e d\Omega \quad (60)$$

3.2. Finite Element Equation of Temperature Field of Coal Containing Gas

In this thesis, the partial differential equation of transient heat conduction can be solved by the finite element method in the airspace and the post difference method in the time domain. The Galerkin method can be used to simplify the differential equation problem to solve the linear equations by the variational principle of the corresponding functional of the equation.

The Finite Element Equation of the Transient Temperature Field

Assuming that the temperature field $T(x, y, z, t)$ is satisfied, the formula (44), owing to $\varphi\rho c_g$, is very small relative to $\rho_s c_s$, so it can be ignored. Therefore, the temperature field Equation (44) can be written as:

$$\rho_s c_s \frac{\partial T}{\partial t} + T \alpha_s K \frac{\partial \varepsilon_V}{\partial t} - \rho c_p \frac{k}{\mu_g} \left(1 + \frac{0.95k^{-0.33}}{p}\right) \nabla p \nabla T - \rho c_p T \left[\frac{k}{\mu_g} \left(1 + \frac{0.95k^{-0.33}}{p}\right) \cdot \nabla^2 p + \left(1 + \frac{0.95k^{-0.33}}{p}\right) \frac{\nabla p \cdot \nabla k}{\mu_g}\right] - k_t \nabla^2 T + \frac{q_{st} a b c p_n}{(1+bp)^2 RT} \frac{\partial p}{\partial t} = Q_T \tag{61}$$

The equivalent integral weak form is established based on the Galerkin method, and the solution domain Ω is discretized. It is assumed that the temperature field function at any point within the unit can be obtained by interpolation formula, as follows:

$$T = \sum_i^n N_i(x, y, z) T_i(t) \tag{62}$$

where N_i is an interpolating function. When considering the arbitrariness of δT , it can be obtained as

$$C_{(T)} \frac{\partial T}{\partial t} + K_{(T)} T = P_{(T)} \tag{63}$$

The elements of matrix $K_{(T)}$, $C_{(T)}$, and $P_{(T)}$ are assembled by the corresponding matrix elements of each unit, as follows:

$$K_{(T)ij} = \sum_e K_{(T)ij}^e + \sum_e H_{(T)ij}^e + \sum_e J_{(T)ij}^e \tag{64}$$

$$C_{(T)ij} = \sum_e C_{(T)ij}^e \tag{65}$$

$$P_{(T)i} = \sum_e P_{(T)Q_i}^e + \sum_e P_{(T)q_i}^e + \sum_e P_{(T)H_i}^e \tag{66}$$

where, $K_{(T)ij}^e$ is the contribution of the unit to the heat conduction matrix and $H_{(T)ij}^e$ is the modification of the heat transfer matrix by the heat exchange boundary of unit. $J_{(T)ij}^e$ is the modification of heat transfer matrix by unit deformation energy and the heat exchange of gas flow, $C_{(T)ij}^e$ is the contribution of the unit to the heat capacity matrix, $P_{(T)Q_i}^e$ is the temperature load that is generated by element heat source and adsorption and desorption heat, $P_{(T)q_i}^e$ is the temperature load of the given heat flow boundary of the unit, and $P_{(T)H_i}^e$ is the temperature load of the heat convection boundary of the unit. The matrix elements of these units are given by the following formula

$$K_{(T)ij}^e = \int_{\Omega} k_t \nabla N_i \nabla N_j d\Omega = \int_{\Omega} k_t \left(\frac{\partial N_i}{\partial x} \frac{\partial N_j}{\partial x} + \frac{\partial N_i}{\partial y} \frac{\partial N_j}{\partial y} + \frac{\partial N_i}{\partial z} \frac{\partial N_j}{\partial z} \right) d\Omega \tag{67}$$

$$H_{(T)ij}^e = \int_{\Gamma_3} h N_i N_j d\Gamma \tag{68}$$

$$J_{(T)ij}^e = \int_{\Omega} \left[\alpha_s K \frac{\partial \varepsilon_V}{\partial t} N_i N_j - \frac{\rho c_p}{\mu_g} \left(1 + \frac{0.95k^{-0.33}}{p}\right) (k \nabla^2 p + \nabla p \cdot \nabla k) N_i N_j + \rho c_p \frac{k}{\mu_g} \left(1 + \frac{0.95k^{-0.33}}{p}\right) \nabla p \nabla N_i N_j \right] d\Omega \tag{69}$$

$$C_{(T)ij}^e = \int_{\Omega} \rho_s c_s N_i N_j d\Omega \tag{70}$$

$$P_{(T)Q_i}^e = \int_{\Omega} (Q_T N_i + N_i \frac{q_{st} abc p_n}{(1+bp)^2 RT} \frac{\partial p}{\partial t}) d\Omega \quad (71)$$

$$P_{(T)q_i}^e = \int_{\Gamma_2} q_t N_i d\Gamma \quad (72)$$

$$P_{(T)H_i}^e = \int_{\Gamma_3} h T_a N_i d\Gamma \quad (73)$$

3.3. Finite Element Equation of Gas Seepage

The Galerkin method is used to deduce the finite element equation of gas seepage field, similar to the method of deducing finite element equation of transient heat conduction. Both sides of the coal-bed methane motion differential Equation (34) are multiplied by $\delta p = \sum N_i \delta p_i$, which meets the coercive boundary conditions. Therefore, we can gain the equation, as

$$\int_{\Omega} \delta p \left\{ \left[\varphi + \frac{abc p_n}{(1+bp)^2} \right] \frac{\partial p}{\partial t} + p \frac{\partial \varphi}{\partial t} - \frac{k}{\mu_g} \nabla p \nabla p - (p + 0.95 \cdot 0.67 k^{-0.33}) \frac{\nabla k \nabla p}{\mu_g} \right. \\ \left. - \left[\frac{D_f^{eff} abc p_n}{(1+bp)^2} + p \frac{k}{\mu_g} + 0.95 \frac{k^{0.67}}{\mu_g} + D_k^{eff} \right] \nabla^2 p \right\} d\Omega = 0 \quad (74)$$

The simplification of the Equation (71) can be written as

$$C_{(G)} \frac{\partial P}{\partial t} + K_{(G)} P = P_{(G)} \quad (75)$$

The elements of matrix $K_{(G)}$, $C_{(G)}$, and $P_{(G)}$ are assembled by the corresponding matrix elements of each unit

$$K_{(G)ij} = \sum_e K_{(G)ij}^e \quad (76)$$

$$C_{(G)ij} = \sum_e C_{(G)ij}^e \quad (77)$$

$$P_{(G)i} = \sum_e P_{(G)i}^e \quad (78)$$

where $K_{(G)ij}^e$ is the contribution of the unit to the mass conduction matrix, $C_{(G)ij}^e$ is the contribution of the unit to the gas storage matrix, and $P_{(G)i}^e$ is the seepage load of a given flow boundary of a unit. The matrix elements of these units are given by the following equations.

$$K_{(G)ij}^e = \int_{\Omega} \left[\left(\frac{D_f^{eff} abc p_n}{(1+bp)^2} + \frac{k}{\mu_g} (p + 0.95 k^{-0.33}) + D_k^{eff} \right) \nabla N_i \nabla N_j - \left(\frac{2D_f^{eff} ab^2 c p_n}{(1+bp)^3} - \frac{k}{\mu_g} \right) N_i \nabla N_j \right] d\Omega \\ - \int_{\Omega} 0.95 \cdot 0.67 \frac{k^{-0.33}}{\mu_g} \nabla k \nabla N_i N_j d\Omega \quad (79)$$

$$C_{(G)ij}^e = \int_{\Omega} \left(\frac{abc p_n}{(1+bp)^2} + \varphi \right) d\Omega \quad (80)$$

$$P_{(G)i}^e = \int_{\Omega} \left(-p N_i \frac{\partial \varphi}{\partial t} \right) d\Omega \quad (81)$$

4. Numerical Simulation of Gas Drainage by Borehole Injection Heat

4.1. Numerical Model

The B10 coal seam of the Xinzhuangzi Coal Mine in China is the outburst coal seam. Thickness of coal seam is 1.0–1.7 m. The inclination angle of coal seam is 20° – 28° . The maximum gas pressure is 1.8 MPa and the gas content is 7–9 m^3/t . The initial permeability of coal seam is $2 \times 10^{-18} \text{ m}^2$. The coal seams that correspond to the overlying B11b coal seam and the underlying B8 coal seam are all outburst coal seams. First, the B10 coal seam is used as a protective layer to the mine. The floor roadway is applied to drill hole, and the strip type pre-drainage gas of coal seam to shield tunnel. The normal distance between the floor roadway and the B10 coal seam is about 12 m and the length is 1100 m. According to the geological conditions of coal mine, the three-dimensional finite element model is established and is shown in Figure 2. As shown in the figure, the coal seam tendencies is 30 m, the coal seam direction is 30 m, the vertical direction is 21.8 m, the coal seam thickness is 1.8 m, the roof thickness is 8 m, and the floor thickness is 12 m. The stress field at the top of the model is applied to 12.8 MPa to simulate the initial stress field from the overburden weight, the initial gas pressure in the coal seam is 1.8 MPa, and the diameter of the drilling hole is 94 mm.

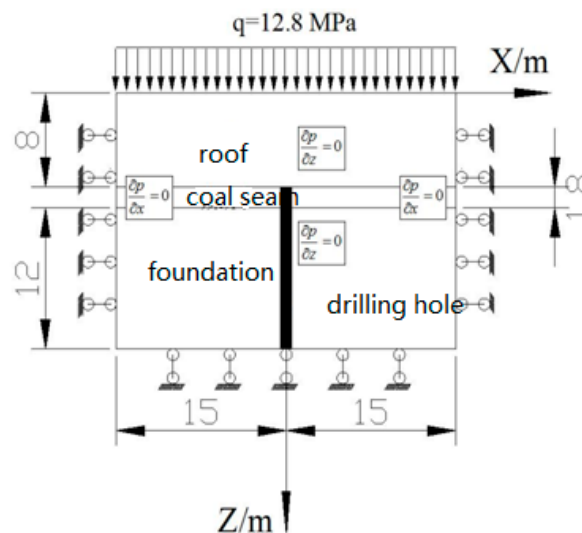


Figure 2. The numerical model.

At present, Salmachi [8] proposed the thermal stimulation method for coal seam by using geothermal water. Shahtalebi [16] studied the thermal stimulation technology for coal seam by the electric resistance method. Wang [15] proposed the thermal stimulation method for coal seam by high temperature nitrogen. There are also many projects that use high temperature steam to thermally stimulate coal seams. The modeling size is large since the three-dimensional mechanical model is established in this paper, which also leads to a large computational workload. This paper does not consider the convective heat transfer process between the heat source and the borehole wall of the coal seam in order to simplify the mechanical model. Instead, the constant temperature boundary condition near the extraction hole is given to simulate the temperature of the injection medium. The temperature changes of coal and coal-bed methane at different coordinate positions from the borehole boundary are calculated according to the temperature field control equation when considering the influence of gas desorption on temperature. Since the specific heat of coal is 1.00 to 1.26 $\text{kJ}/(\text{kg}\cdot\text{K})$, the energy that is required to heat 1 ton of coal by 1 degree Celsius is about 1.0–1.26 MJ.

The models with constant temperature boundaries of 350 K, 375 K, and 400 K are, respectively, set up for calculation and analysis. Table 1 shows the numerical simulation scheme for gas extraction by

heat injection. Table 2 shows the material parameters of all strata. For ease of understanding, Table 3 shows the conversion between international units and common units of each variable.

Table 1. Numerical simulation scheme for heat injection.

Different temperature	Model 1:350 K Model 2:375 K Model 3:400 K
Different coefficient of thermal expansion	Model 1: $1 \times 10^{-7} \text{ K}^{-1}$ Model 2: $5 \times 10^{-7} \text{ K}^{-1}$ Model 3: $1 \times 10^{-6} \text{ K}^{-1}$

Table 2. Mechanical parameters of each rock stratum.

Strata Formation Name	Thickness h/m	Elastic Modulus E/GPa	Poisson Ratio	Internal Cohesion /MPa	Internal Friction angle /($^{\circ}$)	Tensile Strength /MPa	Density / $\text{kg}\cdot\text{m}^3$
roof	8	5.89	0.16	3.2	40.9	3.7	2721
Coal seam	1.8	2.4	0.29	0.2	20	0.28	1450
foundation	12	5.89	0.16	3.2	40.9	3.7	2721

Table 3. Common unit conversion table.

Length variable	1 m = 3.281 feet
Gas production	1 m^3 = 1000 L = 6.29 bbl
Temperature	1 K = 1 $^{\circ}\text{C}$ + 273.15
Quality	1 t = 1000 kg
Permeability	1 m^2 = 1.013×10^{15} md
Pressure	1 MPa = 10^6 Pa

4.2. Effect of Heat Injection Temperature on Gas Production Efficiency

The temperature of injection heat will affect the ability of gas occurrence and diffusion. It can also affect the rate of gas production and the total gas production. In this paper, the mechanical models for injection heat temperature of 350 K, 375 K, and 400 K are calculated and analyzed, respectively. Figure 3 shows the variation curves of the gas production rate with the time of injection heat at different injection temperatures. Figure 4 shows the variation curves of total gas production with the time of injection heat at different injection temperatures. Both of them are compared with the field data that are measured without heat injection [33].

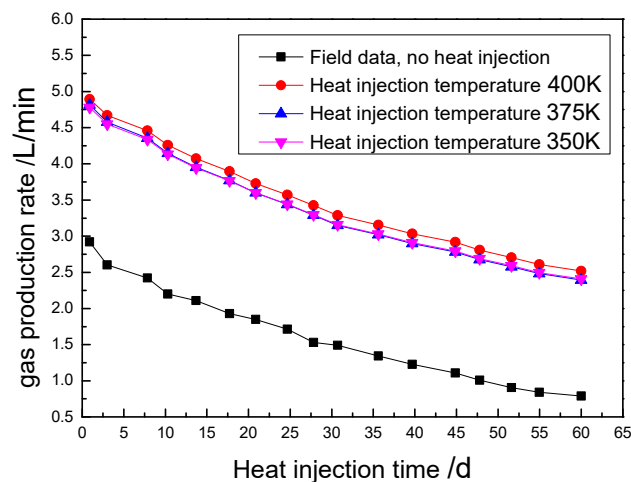


Figure 3. Effect of heat injection temperature on gas production rate.

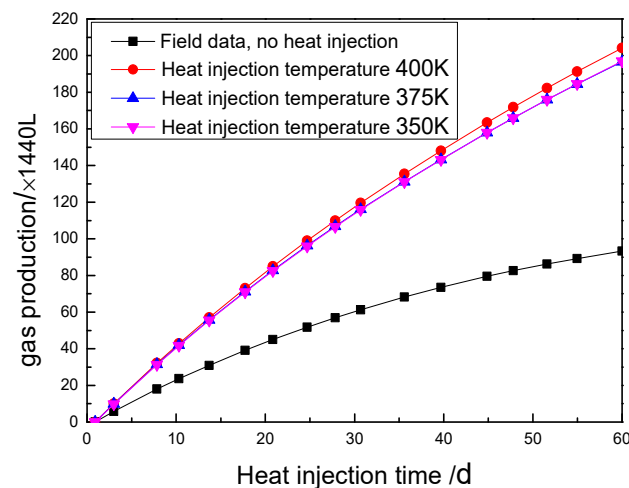


Figure 4. Effect of heat injection temperature on total gas production.

According to the Figure 3, when the injection temperatures are 400 K, 375 K, and 350 K, respectively, the gas production rates are 4.8944 L/min., 4.817 L/min., and 4.780 L/min at the initial stage of extraction. These data increased significantly compared with field data 2.920 L/min. with initial temperatures 300 K. The increase amplitudes are 67.62%, 64.95% and 63.69% respectively. When the mining period is 30 days, the gas production rates are 3.286 L/min., 3.159 L/min., and 3.150 L/min. of the injection temperatures 400 K, 375 K, and 350 K, respectively. The number increased more significantly when compared with field data 1.49 L/min. with the initial temperature 300 K. The increase amplitudes are 120.5%, 112%, and 111.4%, respectively. Therefore, we can see that the injection heat can obviously increase the gas production rate. In addition, the influence of injection heat on the increase of gas production is also significant with the development of mining. Figure 4 shows that the injection heat can effectively increase gas production, when the mining period is 30 days, the total gas production are 172,201.54 L, 167,158.66 L, and 166,792.9 L of the injection temperatures 400 K, 375 K, and 350 K, respectively. It increased more significantly when compared with field data 88,204.55 L with initial temperature 300 K, and the increase rate of coal-bed methane is 95.23%, 89.5%, and 89.09%, respectively. When the mining period is 60 days, the total gas productions are 293,939.57 L, 283,532.69 L, and 283,321.01 L of the injection temperatures 400 K, 375 K, and 350 K, respectively. The increase rates of coal-bed methane are 118.8%, 110.09%, and 110.08%, respectively. With the increase of injection heat time from 30 d to 90 d, the increase rate of coal-bed methane increased from 90% to 110%. With the heat injection temperature increase from 350 K to 400 K, the gas production gradually increased, but the change is a little.

4.3. The Influence of Injection Heat Temperature on the Distribution of Gas Pressure

From the mechanism of gas migration, we can see that temperature rise can promote the desorption of gas, so the adsorbed gas can be transformed into free gas. In addition, temperature is an important factor that affects gas diffusion. The Fick diffusion coefficient and Knudsen diffusion coefficient of gas in large meso-pore are related to temperature. The influence of heat injection on gas pressure relief is discussed in order to study the distribution and evolution rule of coal seam gas pressure under different injection temperature. The distribution rule of gas pressure around the borehole at different injection temperatures is calculated and analyzed after the 30-day gas extraction, as shown in Figures 5–7.

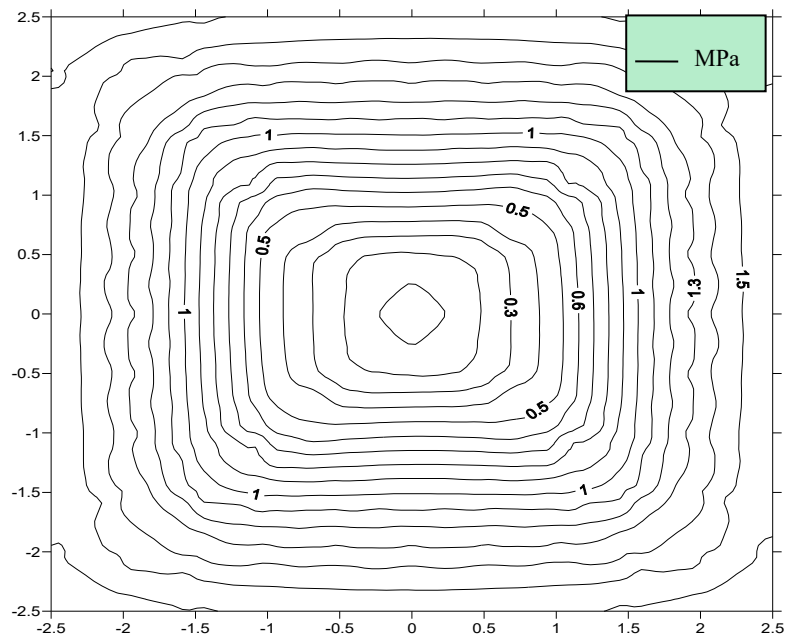


Figure 5. When $T = 350$ K, the distribution of gas pressure around boreholes.

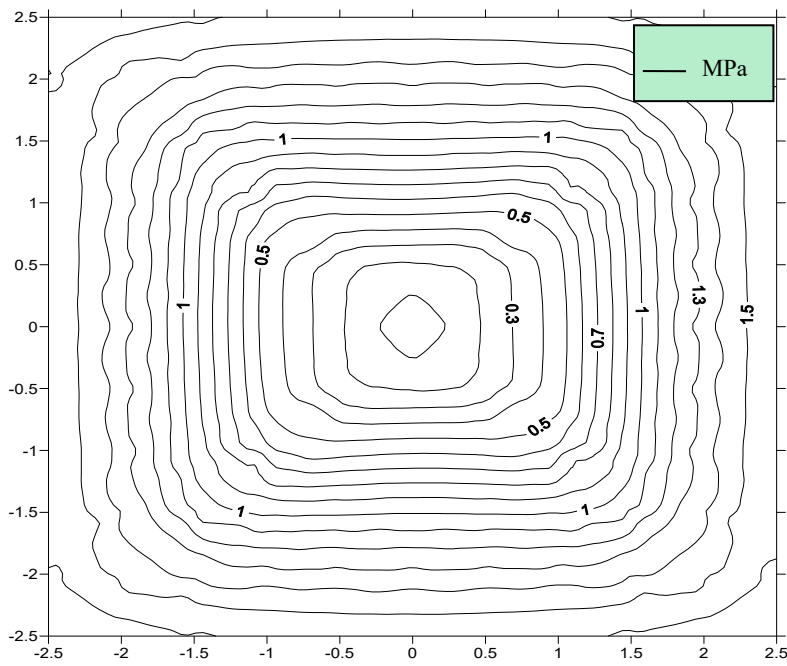


Figure 6. When $T = 375$ K, the distribution of gas pressure around boreholes.

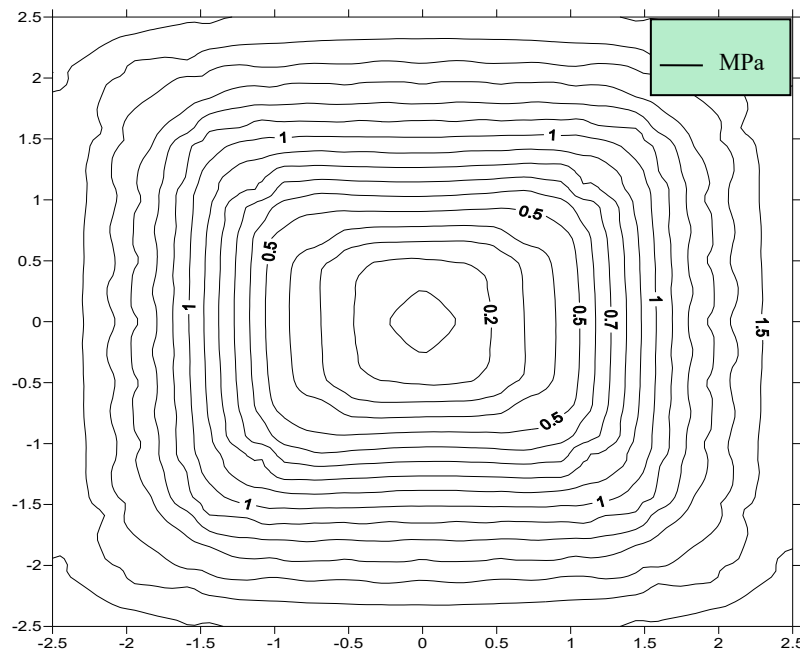


Figure 7. When $T = 400\text{ K}$, the distribution of gas pressure around boreholes.

From Figures 5–7, we can see that, the closer the distance to the borehole is, the smaller the gas pressure is, and the more obvious the pressure relief is. With the increase of gas drainage time, the gas pressure around boreholes will also gradually decrease. We recorded the gas pressure changes at 1 m and 2 m away from borehole in order to study the effects of injection heat temperature (350 K, 375 K, 400 K) on the gas pressure relief, respectively. The evolution rule of gas pressure with drainage time is obtained, as shown in Figures 8 and 9. Figure 10 shows the effect of injection heat temperature on effective drainage radius.

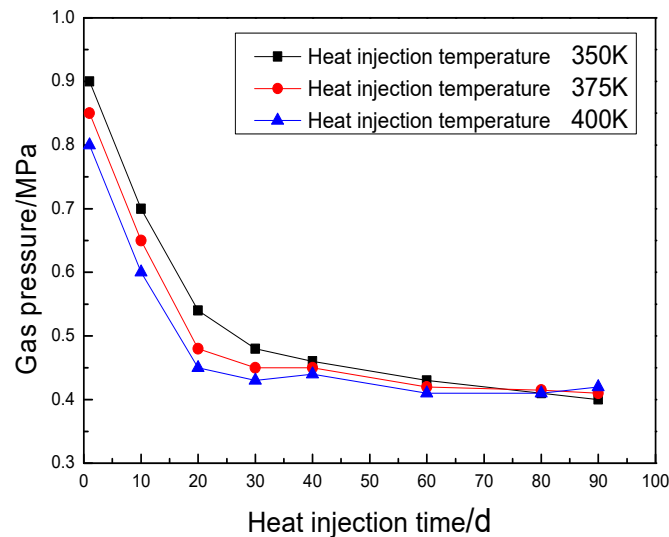


Figure 8. The variation curve of gas pressure with the drainage time at 1 m away from the borehole.

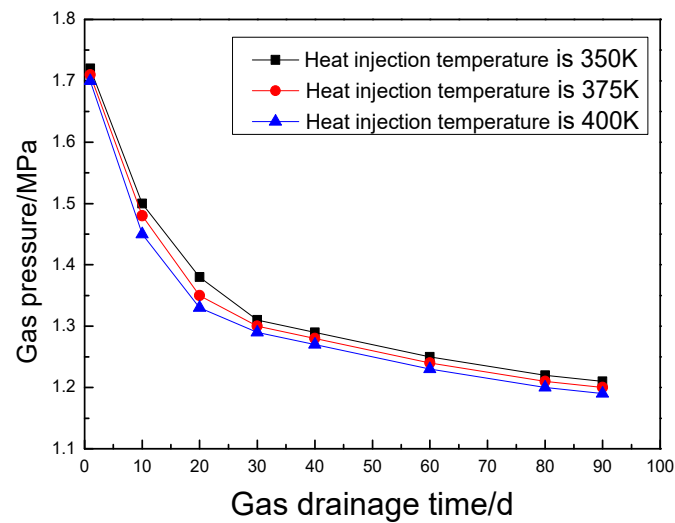


Figure 9. The variation curve of gas pressure with the drainage time at 2 m away from the borehole.

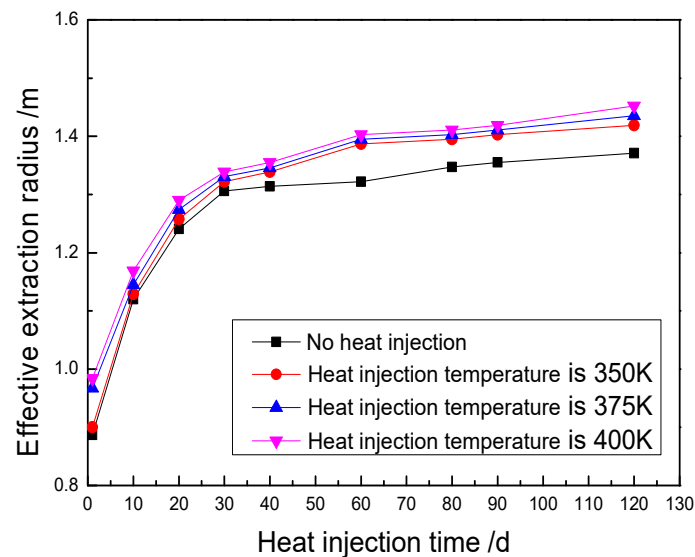


Figure 10. Effect of heat injection temperature on effective extraction radius.

Under the action of injection heat, the coal seam temperature increases and the gas diffusion capacity increases. The theoretical analysis shows that the gas Fick diffusion coefficient and the Knudsen diffusion coefficient, respectively, relates to the 1.5 and the 0.5 power of the temperature. It also illustrates that the rise of temperature can effectively increase the diffusion coefficient of gas. As shown in Figure 8, after 60 days of gas extraction, when the injection heat temperature increases from 350 K to 375 K and 400 K, the gas pressure decreases from 1.8 MPa to 0.43 MPa, 0.42 MPa, and 0.41 MPa at 1 m away from borehole, respectively. From Figure 9, we know that, under the same circumstances, the gas pressure decreases from 1.8 MPa to 1.25 MPa, 1.24 MPa, and 1.23 MPa at 2 m away from the hole, respectively. The decline range of gas pressure at 1 m distance from the drill hole is larger than that at 2 m distance from the drill hole.

Figure 10 shows the influence curve of injection heat temperature on effective extraction radius of the borehole, as the effective extraction radius of borehole is an important index for gas outburst elimination. From Figure 10, we can see that injection heat can increase the effective extraction radius of boreholes. The rise of temperature is favorable for the desorption and diffusion of gas. Injection heat can also increase the range of gas pressure relief. For example, the effective extraction radius of the borehole is 1.31 m without injection heat after 60 days of gas drainage. When the injection

heat temperature is 350 K, 375 K and 400 K, the effective extraction radius is 1.38 m, 1.395 m, and 1.41 m, respectively, and the effective extraction radius is increased when compared with that without heat injection.

4.4. Effects of the Thermal Expansion Coefficient on Gas Production

The thermal expansion coefficient of coal seam has great influence on its thermal expansion deformation. The effects of different thermal expansion coefficients on gas production efficiency are studied in this section. Figure 11 shows the influence curves of different the thermal expansion coefficients on gas production rate.

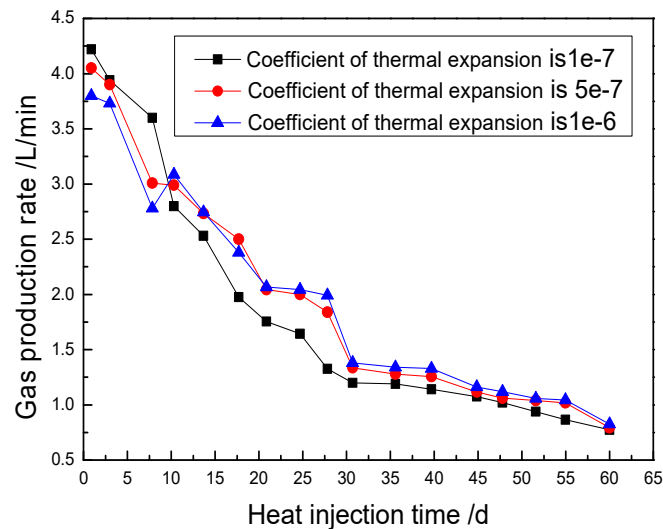


Figure 11. Effect of different thermal expansion coefficient on gas production rate.

As seen from Figure 11, in the first eight days of mining, when the thermal expansion coefficient of coal seam increases from 10^{-7} to 5×10^{-7} , and 10^{-6} , the gas production rate decreases from 4.22 L/min., 4.05 L/min., and 3.8 L/min. to the 3.6 L/min., 3.008 L/min., and 2.78 L/min., respectively. When the injection time exceeds 10 days, the gas production rate increases with the increase of thermal expansion coefficient of the coal seam. When the gas is extracted for 28 days, the gas production rate of the coal seam with the thermal expansion coefficient 5×10^{-7} and 10^{-6} are the 1.84 L/min, and 1.992 L/min., respectively, which is much larger than that of the coal seam with the thermal expansion coefficient 10^{-7} , and the increase range is 38.7% and 50.2%, respectively. Some changes will occur as the coefficient of thermal expansion changes according to the effective stress theory of coal body and the evolution theory of coal seam porosity and permeability. On the one hand, as the coefficient of thermal expansion increases, the thermal stress increases, the effective stress decreases, the pores of coal seam expand, and gas desorption reduces the pore pressure and temperature, the effective stress increases, and the pore space of coal seam decreases. On the other hand, as the coefficient of thermal expansion increases, the inward thermal expansion deformation of coal seam increases, and the pore space is reduced, as the gas pressure and temperature decrease, the inward adsorption deformation and temperature strain decrease, and the pore space increases. The former makes the permeability of coal seam increase first and then decreases, while the latter makes the permeability of coal seam decrease first and then increase, resulting in the trend that the gas production rate first decreases and then increases.

5. Conclusions

The main research contents and conclusions of this paper are summarized, as follows:

- (1) When considering the effects of the temperature, the gas migration and the redistribution of mining stress comprehensively, this paper proposes using the effective strain field to define the damage field of the coal body. This variable is a quantitative description for the degree of coal rupture and damage. A new mathematical model of coal damage-heat-gas-solid multi-field coupling is developed.
- (2) Based on the multi-physical field coupling theory that was established in this paper, according to the numerical solution method, the finite element source program is developed twice by using FORTRAN language, and the multi-field coupling analysis program is compiled when considering temperature, gas seepage, damage, and deformation of coal and rock. Subsequently, it was applied for the analysis of borehole thermal stimulation for coal-bed methane mining. The results show that, when the injection heat temperature increased from 350 K to 400 K, the rate of gas production and total gas production increased by more than 110% and 90%, respectively. As gas drainage is carried out, the efficiency of gas production is gradually increased. When the drainage time changed from 30 d to 90 d, the total gas production increased from 90% to 110%, and the amount of gas production significantly increased.
- (3) The thermal stimulation of boreholes caused the rise of coal seam temperature, which promoted the decrease of gas pressure and the increase of the effective extraction radius of boreholes. For example, when the gas is extracted for 60 days, the effective extraction radius without heat injection is 1.31 m. When the injection temperatures are 350 K, 375 K, and 400 K, the effective extraction radius are 1.38 m, 1.395 m, and 1.41 m, respectively. The thermal expansion coefficient of coal seam has significant effect on the gas production rate of coal-bed methane. The main reason is that the thermal expansion coefficient changes the effective stress of coal body and the inward thermal expansion deformation of coal pores. The former factor makes the permeability of coal seam increase first and then decrease, while the latter makes the permeability of coal seam decrease first and then increase, resulting in the trend that the gas production rate first decreases and then increases.
- (4) In this paper, the effect of coal fracture and damage on the deformation of solid structure and gas migration is investigated, and the paper has made great progress when compared with previous studies. This paper utilizes the damage variable to describe the development of coal fracture since the finite element theory adopted is based on the continuous mechanics. Whereas, the development and expansion of multiple fractures of coal body under the action of multiple physical fields cannot be accurately studied. To simplify the mechanical model, the gas-liquid two-phase flow that occurred during the heat injection process has not been considered, which poses a great challenge to our future work.

To sum up, these obtained results can provide significant theoretical guidance for the design of gas drainage and the improvement of the efficiency of gas extraction.

Author Contributions: This research work is completed by five people. H.C. is responsible for the writing and revision of the paper, N.Z. is responsible for the programming and calculation, W.P. is responsible for the data curation, H.C. was responsible for the investigation research work, the cost of the study is funded by Y.Y.

Funding: This research received no external funding.

Acknowledgments: This work was supported by the Fundamental Research Funds for the Central Universities (2019XKQYMS41).

Conflicts of Interest: The authors declare that there is no conflict of interests regarding the publication of this article.

References

- Kang, J.; Zhou, F.; Qiang, Z.; Zhu, S. Evaluation of gas drainage and coal permeability improvement with liquid CO₂ gasification blasting. *Adv. Mech. Eng.* **2018**, *10*. [[CrossRef](#)]
- Puri, R.; Yee, D. Enhanced Coalbed Methane Recovery. *Soc. Pet. Eng. AIME* **1990**, *65*, 193–202.
- Syed, A.; Shi, J.Q.; Durucan, S. Permeability and injectivity improvement in CO₂ enhanced coalbed methane recovery: Thermal stimulation of the near wellbore region. *Energy Procedia* **2011**, *4*, 2137–2143. [[CrossRef](#)]
- Cai, Y.D.; Liu, D.M.; Liu, Z.H.; Zhou, Y.F.; Che, Y. Evolution of pore structure, submaceral composition and produced gases of two Chinese coals during thermal treatment. *Fuel Process. Technol.* **2016**, *156*, 298–309. [[CrossRef](#)]
- Yang, R.T.; Saunders, J.T. Adsorption of gases on coals and heat treated coals at elevated temperature and pressure: 1. Adsorption from hydrogen and methane as single gases. *Fuel* **1985**, *64*, 616–620. [[CrossRef](#)]
- Lin, Y.B.; Ma, D.M.; Liu, Y.H. Experiment of the influence of temperature on coalbed methane adsorption. *Coal Geol. Explor.* **2012**, *40*, 24–28.
- Zhou, S.N.; Lin, B.Q. *Coal Seam Gas Occurrence and Flow Theory*; China Coal Industry Press: Beijing, China, 1999.
- Salmachi, A.; Haghighi, M. Feasibility study of thermally enhanced gas recovery of coal seam gas reservoirs using geothermal resources. *Energy Fuels* **2012**, *26*, 5048–5059. [[CrossRef](#)]
- Cheraghian, G. A new thermal method concept for IOR from oil reservoir using optimized in-situ combustion. In Proceedings of the 78th EAGE Conference and Exhibition, Vienna, Austria, 30 May–2 June 2016.
- Wang, H.Y.; Ajao, O.; Economides, M.J. Conceptual study of thermal stimulation in shale gas formations. *J. Nat. Gas Sci. Eng.* **2014**, *21*, 874–885. [[CrossRef](#)]
- Wong, T.F.; Brace, W.F. Thermal expansion of rocks: Some measurements at high pressure. *Tectonophysics* **1979**, *57*, 95–117. [[CrossRef](#)]
- Akbarzadeh, H.; Chalaturnyk, R.J. Structural changes in coal at elevated temperature pertinent to underground coal gasification: A review. *Int. J. Coal Geol.* **2014**, *131*, 126–146. [[CrossRef](#)]
- Zhu, W.C.; Wei, C.H.; Liu, J.; Qu, H.Y.; Elsworth, D. A model of coal-gas interaction under variable temperatures. *Int. J. Coal Geol.* **2011**, *86*, 213–221. [[CrossRef](#)]
- Li, Z.Q.; Xian, X.F.; Long, Q.M. Experiment study of coal permeability under different temperature and stress. *J. China Univ. Min. Technol.* **2009**, *38*, 523–527.
- Wang, S.; Zhou, F.; Kang, J.; Wang, X.; Li, H.; Wang, J. A heat transfer model of high-temperature nitrogen injection into a methane drainage borehole. *J. Nat. Gas Sci. Eng.* **2015**, *24*, 449–456. [[CrossRef](#)]
- Shahtalebi, A.; Khan, C.; Dmyterko, A.; Shukla, P.; Rudolph, V. Investigation of thermal stimulation of coal seam gas fields for accelerated gas recovery. *Fuel* **2016**, *180*, 301–313. [[CrossRef](#)]
- Qian, J.; Zhou, J. Two damage models of concrete and its application. *J. Hohai Univ.* **1989**, *3*, 40–47.
- Mazars, J.; Boerman, D.J.; Piatti, G. Mechanical damage and fracture of concrete structure. In Proceedings of the 5th International Conference on Fracture (ICF5), Cannes, France, 29 March–3 April 1981.
- Wu, G.; Sun, J.; Wu, Z. Damage mechanical analysis of unloading failure of intact rock mass under complex stress state. *J. Hohai Univ.* **1997**, *25*, 46–51.
- Wu, S.Y.; Guo, Y.Y. Study on the movement property of coal seam methane. *J. China Coal Soc.* **1999**, *24*, 65–69.
- Wu, Y.; Liu, J.; Chen, Z.; Elsworth, D.; Pone, D. A dual poroelastic model for CO₂-enhanced coalbed methane recovery. *Int. J. Coal Geol.* **2011**, *86*, 177–189. [[CrossRef](#)]
- Zhang, H.; Liu, J.; Elsworth, D. How sorption-induced matrix deformation affects gas flow in coal seams: A new FE model. *Int. J. Rock Mech. Min. Sci.* **2008**, *45*, 1226–1236. [[CrossRef](#)]
- Carman, P.C. *Flow of Gases through Porous Media*; Academic Press: New York, NY, USA, 1956.
- Ye, Z.; Chen, D.; Wang, J.G. Evaluation of the non-Darcy effect in coalbed methane production. *Fuel* **2014**, *121*, 1–10. [[CrossRef](#)]
- Cai, J.C. A fractal approach to low velocity non-Darcy flow in a low permeability porous medium. *Chin. Phys. B* **2014**, *24*, 385–389. [[CrossRef](#)]
- Nie, B.S.; He, X.Q.; Wang, E.Y. The diffusion mechanism and model of gas in coal seam. *China Saf. Sci. J.* **2000**, *10*, 24–28.
- Peter Luo, Y. *Methane Emission from Coal Mine*; China Coal Industry Publishing House: Beijing, China, 1983.
- Roy, S.; Raju, R.; Chuang, H.F.; Cruden, B.A.; Meyyappan, M. Modeling gas flow through micro channels and nanopores. *J. Appl. Phys.* **2003**, *93*, 4870–4879. [[CrossRef](#)]

29. Jones, F.O.; Owens, W.W. A laboratory study of low-permeability gas sands. *J. Pet. Technol.* **1980**, *32*, 1631–1640. [[CrossRef](#)]
30. Chen, X.Z.; Zhang, L.P. Numerical analysis for the influence of temperature field on coalbed methane migration by gas injection. *J. Min. Saf. Eng.* **2014**, *31*, 803–808.
31. Teng, T. Mechanism of Heat-Moisture-Fluid-Solid Interactions in Coal Seam Gas Recovery. Ph.D. Thesis, China University of Mining and Technology, Xuzhou, China, 2017.
32. Dai, Y.; Chen, W.; Wu, G.; Zhou, X. Study on elastoplastic damage model of unsaturated rock mass and its application. *J. Rock Mech. Eng.* **2008**, *4*, 728–735.
33. Yu, T.; Lu, P.; Sun, J.; Deng, Z. Measurement of effective drainage radius based on gas flow and pressure of boreholes. *J. Min. Saf. Eng.* **2012**, *4*, 596–600.



© 2019 by the authors. Licensee MDPI, Basel, Switzerland. This article is an open access article distributed under the terms and conditions of the Creative Commons Attribution (CC BY) license (<http://creativecommons.org/licenses/by/4.0/>).